

Negative magnetoresistance in the c -axis resistivity of $\text{Bi}_2\text{Sr}_2\text{CaCu}_2\text{O}_{8+\delta}$ and $\text{YBa}_2\text{Cu}_3\text{O}_{6+x}$

Y. F. Yan, P. Matl, J. M. Harris, and N. P. Ong

Joseph Henry Laboratories of Physics, Princeton University, Princeton, New Jersey 08544

(Received 13 March 1995)

The c -axis resistivity ρ_c in $\text{Bi}_2\text{Sr}_2\text{CaCu}_2\text{O}_{8+\delta}$ and oxygen-reduced $\text{YBa}_2\text{Cu}_3\text{O}_{6+x}$ is quite sensitive to a magnetic field \mathbf{H} . The magnetoresistance (MR) is large (1% at 14 T and 100 K), weakly anisotropic, and negative over a wide range of temperatures T above the critical temperature T_c . The magnitude of the MR is activated in temperature with a characteristic energy U_L that varies with the oxygen content δ . We interpret the activated form of ρ_c and the negative MR in terms of a pseudogap Δ that is slightly reduced by H .

A distinctive property of the cuprate superconductors is their anisotropic electrical resistivity at temperatures T above the superconducting critical temperature T_c . In the underdoped regime, the c -axis resistivity ρ_c displays an insulating trend (increases as T decreases) while the in-plane resistivity ρ_{ab} is "metallic" in behavior.¹⁻³ In $\text{Bi}_2\text{Sr}_2\text{CaCu}_2\text{O}_{8+\delta}$ (Bi 2212), which has an anisotropy ρ_c/ρ_a in the range 10^4 – 10^5 , the insulating trend is observable as high as 200 K, even in the overdoped regime. Recently, evidence suggestive of a pseudogap in underdoped $\text{YBa}_2\text{Cu}_3\text{O}_{6+x}$ (YBCO) was obtained from resistivity,^{4,5} specific heat,⁶ and reflectivity measurements.⁷ Less evidence has been obtained for Bi 2212. However, the bilayer coupling is expected to play a role similar to that in YBCO.^{8,9}

To clarify further the c -axis conduction, we have studied in detail the effect of a magnetic field \mathbf{H} (or \mathbf{B}) on ρ_c in four crystals of $\text{Bi}_2\text{Sr}_2\text{CaCu}_2\text{O}_{8+\delta}$ (Bi 2212) grown by the self-flux method. By powder x-ray diffraction, we can exclude the 2223 and 2201 phases. After growth, the oxygen content δ was altered by annealing in either Ar or O_2 atmosphere at the anneal temperatures T_a given in Table I (δ increases in the sequence A,B,C,D). While the effect of δ on ρ_{ab} has been studied extensively,¹⁰ less is known about its effect on the magnetoresistance (MR) of ρ_c . We also study one crystal of $\text{YBa}_2\text{Cu}_3\text{O}_{6.7}$ (YBCO_{6.7}) with $T_c(0) = 65$ K. To obtain the 60-K phase, we sealed an as-grown 90-K crystal in a quartz tube together with ceramic YBCO and annealed for 7 days at 500 °C. For the MR experiment, the field dependence of the regulating thermometer was carefully measured [cernox (Lakeshore 1050) has a negative MR that varies from 1 in 10^{-6} at 150 K to 1 in 10^{-7} at 300 K at 1 T]. All MR measurements were corrected for the field dependence of the sensor.

The temperature profiles of the normal-state ρ_c in the crystals are displayed in Fig. 1. In the Bi 2212 crystals with highest oxygen content δ (C and D), ρ_c shows a broad minimum at a temperature we will call T_{\min} . With decreasing δ , T_{\min} moves rapidly to higher T (in A and B, T_{\min} lies above 400 K). In YBCO_{6.7}, ρ_c is about a factor of 10 smaller (inset). However, its profile is similar, with T_{\min} higher than 300 K. The solid lines are fits discussed later. In the mixed state below T_c , a 14-T field ($\mathbf{H}\parallel c\parallel z$) leads to a large flux-flow resistivity ρ_{zz} as displayed in Fig. 2. As reported previously,^{11,12} ρ_{zz} in Bi 2212 seems to follow the extrap-

lation of the normal-state ρ_c curve at temperatures just below T_c . The main panel shows curves taken at 14 T for samples A–D. In the inset we show that the same behavior is evident in YBCO_{6.7}. We note that the fractional increase in ρ_c of YBCO_{6.7} measured at 14 T is comparable to that observed in sample A. However, if we increase δ in Bi 2212, we observe that ρ_{zz} increases to its peak value at a much higher rate (compare samples D and A in the main panel). This uncovers an unexpected trend. While a higher oxygen content lowers the overall magnitude of ρ_c in the normal state, it simultaneously enhances the rate $|d\rho_c/dT|$ at which ρ_c increases at low temperatures. We attempt to quantify these trends below [Eq. (1)].

A longitudinal field ($\mathbf{H}\parallel\mathbf{J}\parallel c$) has a significant effect on ρ_c in Bi 2212. The fractional change is 2–3 orders of magnitude larger than normally encountered in ordinary metals. It is also negative over a large range of T above T_c . The fractional change of the resistivity $\Delta\rho_c/\rho_c$ is strongly T dependent, growing by a factor of ~ 100 from 220 to 96 K in sample D (Fig. 3). This remarkable growth suggests that the negative MR should be observable below T_c . In the vortex state below T_c , the dominant effect of the field is to induce vortex motion (and in sufficiently intense fields) to destroy phase coherence between adjacent bilayers. Both effects lead to a very large, positive MR. Thus, ρ_{zz} initially rises very rapidly with field. However, in all Bi 2212 crystals, we observe that ρ_{zz} actually attains a maximum and then decreases in higher fields (Fig. 3, inset). A detailed study¹³ shows that

TABLE I. The parameters a , Δ , b , and d [Eq. (1)] and the energy scale U_L (Fig. 4) for samples A, B, C, and D. The first line gives T_a (in °C)/anneal time (in days) (oxygen content increases from A to D). The second line gives the anneal atmosphere (at ambient pressure).

Sample	A	B	C	D
T_a (°C)/time (d)	550/14	550/8	550/8	480/8
Atmos.	Ar	Ar	O_2	O_2
T_c (K)	86	88	84	84
a (Ω cm K)	684 ± 20	94 ± 1.4	7.6 ± 0.1	3.85 ± 0.1
Δ (K)	69 ± 2	240 ± 1	323 ± 0.7	370 ± 1.5
b (m Ω cm/K)	9.5 ± 0.5	0	2.78 ± 0.03	3.26 ± 0.06
d (Ω cm)	5.66 ± 0.2	5.18 ± 0.03	4.43 ± 0.01	4.01 ± 0.02
U_L (K)	256 ± 10	379 ± 14	456 ± 10	392 ± 6

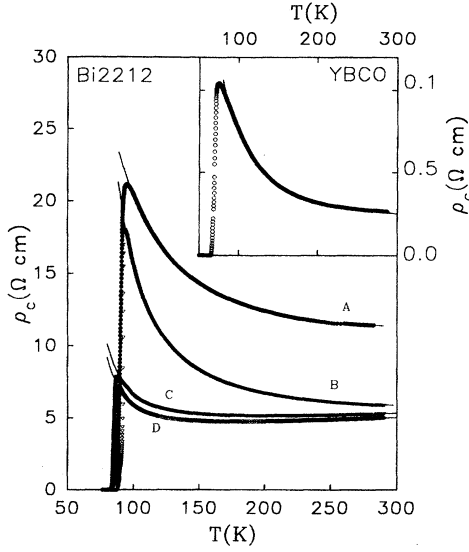


FIG. 1. (Main panel) Temperature dependence of ρ_c in four crystals of $\text{Bi}_2\text{Sr}_2\text{CaCu}_2\text{O}_{8+\delta}$ with different δ (A, B, C, and D). Current electrodes are annular rings painted on the ab face (with Ag epoxy). The voltage contacts are spots painted in the center of the rings. With increasing δ in Bi 2212 (A–D), the overall magnitude of ρ_c decreases monotonically. However the slope $|d\rho_c/dT|$ above T_c increases. The inset shows ρ_c in a crystal of $\text{YBa}_2\text{Cu}_3\text{O}_{6.7}$. Fits to Eq. (1) are shown as solid lines in all curves.

the decrease in high fields is a *continuation* of the negative MR of the normal state. Examination of the inset in Fig. 3 shows that the value of ρ_{zz} at 14 T is significantly lower than the intrinsic normal-state, zero-field value of ρ_c . A similar set of negative MR curves is obtained between 275 and 105 K in the $\text{YBCO}_{6.7}$ crystal.¹³ The MR ($\Delta\rho_c/\rho_c B^2$) changes rapidly from -8×10^{-7} to -7×10^{-6} between the two temperatures.

To quantify the T dependence of the MR, we express $\Delta\rho_c$ in the form $\Delta\rho_c/\rho_c = -[C_L(T)B]^2$. Close to T_c (below 105 K), a second term $-\gamma B \ln B$ (associated with suppression of paraconducting terms¹³) is needed to fit the data (see Fig. 3). Plotted in semilog scale (Fig. 4), C_L in all Bi 2212 samples displays an activated behavior with an energy scale U_L , viz., $C_L = C_{L0} \exp(U_L/T)$ (U_L is given in Table I). To investigate the MR anisotropy, we have also performed measurements with \mathbf{H} rotated into the ab plane keeping $\mathbf{J} \parallel c$ (Fig. 4, inset). Because of the large anisotropy in Bi 2212 ($\rho_c/\rho_{ab} \sim 10^4 - 10^5$), we expected to see a dramatic change in the MR. Instead, the observed MR anisotropy is remarkably weak. At its largest value (just above T_c), the transverse MR coefficient C_T is about a factor of 2 smaller than C_L . With increasing T , the anisotropy decreases and becomes unresolved above ~ 170 K. In the main panel, we have displayed data in $\text{YBCO}_{6.7}$. Unlike in Bi 2212, C_L is not activated in $\text{YBCO}_{6.7}$ (we did not study the anisotropy).

In all the Bi 2212 crystals studied, we find that the MR is invariably negative whenever ρ_c displays a pronounced insulating trend ($d\rho_c/dT < 0$). However, in a strongly overdoped sample G in which $T_{\min} \sim 125$ K, we find that the MR changes from negative below 165 K to positive above (data for G will be reported elsewhere¹³). The sign change occurs

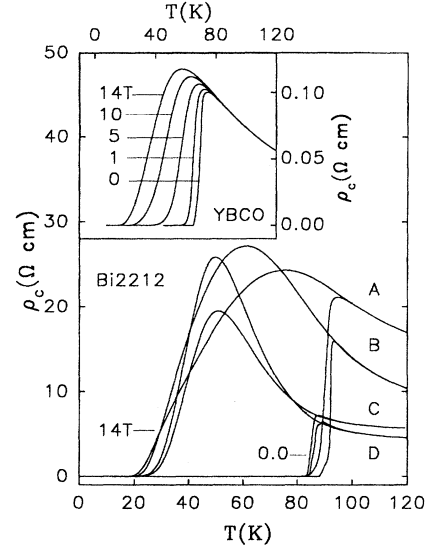


FIG. 2. (Main panel) The flux-flow resistivity ρ_{zz} in $\text{Bi}_2\text{Sr}_2\text{CaCu}_2\text{O}_{8+\delta}$ (samples A, B, C, and D) in a longitudinal field of 14 T ($\mathbf{B} \parallel \mathbf{J} \parallel c$). ρ_{zz} appears to continue the T dependence of the normal-state ρ_c close to T_c , but attains a broad peak at lower T . The relative size of the peak and its position vary with δ . Note that, just below T_c , $|d\rho_{zz}/dT|$ is much larger in D than in A. Curves for ρ_{zz} in $\text{YBa}_2\text{Cu}_3\text{O}_{6.7}$ for B fixed at 0, 1, 5, 10, and 14 T are shown in the inset ($\mathbf{B} \parallel c$).

at a temperature slightly higher than T_{\min} . (In sample D with $T_{\min} = 200$ K, the MR changes sign at 220 K.) In the positive region, the magnitude of $\Delta\rho_c/\rho_c$ in fixed H is non-monotonic in temperature. In sample G it attains a maximum at 325 K.

We may summarize the rich behavior of the c -axis MR in Bi 2212 as follows. At high temperatures, where $d\rho_c/dT > 0$, the MR is positive and varies in magnitude non-monotonically with T . Below T_{\min} , however, the MR becomes negative and follows a steep, activated increase with falling temperature. This strong activation persists below T_c , and is readily apparent in the flux-flow resistivity in the high-field limit. The near coincidence of the onset of the negative MR with T_{\min} suggests that the negative MR behavior is closely associated with the steep increase in ρ_c below T_{\min} . If the steep increase in ρ_c is caused by the opening of a pseudogap Δ , the negative MR implies that a magnetic field decreases the magnitude of the pseudogap. Moreover, comparison of the data taken with $\mathbf{H} \parallel c$ and $\mathbf{H} \perp c$ in the negative MR regime shows that the magnitude is about twice as large in the former ($\mathbf{H} \parallel c$) compared to the latter. The relatively weak anisotropy suggests that the spin degrees of freedom are important in causing both the activated behavior of ρ_c and the negative MR.

We have attempted to quantify the trend for ρ_c shown in Fig. 1. Our data strongly suggest that ρ_c is made up of two components: an activated term and a linear- T term ($bT + d$), viz.,

$$\rho_c(T) = (a/T)e^{\Delta/T} + bT + d, \quad (1)$$

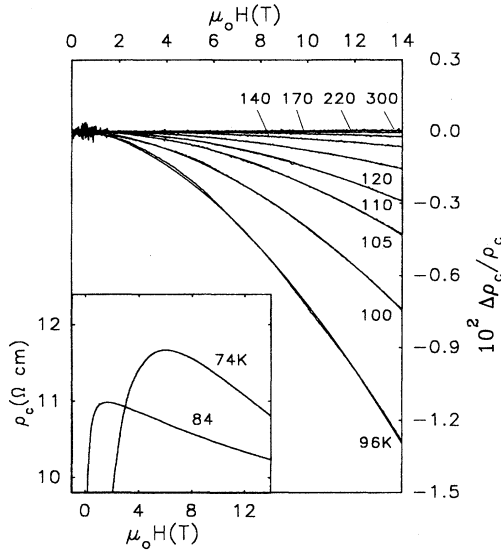


FIG. 3. (Main panel) The magnetoresistance of ρ_c in sample D between 96 and 300 K. Below 220 K, the MR is negative and increases rapidly in magnitude with decreasing T . The fits (smooth lines) have the form $\Delta\rho_c/\rho_c = -[C_L(T)B]^2 - \gamma B \ln B$, with $\gamma = 1.4 \times 10^{-4}$, 5.13×10^{-5} , and $6.45 \times 10^{-6} \text{ T}^{-1}$ at 96, 100, and 105 K (γ is unresolved above 105 K). The nonmonotonic behavior of ρ_{zz} is shown in the inset. The high-field decrease (which persists to 28 T) is an extension of the negative MR in the main panel to temperatures below T_c .

(a , b , and d are T independent). We find that Eq. (1) fits the measured ρ_c in Bi 2212 and YBCO_{6,7} surprisingly well. The fit parameters are given in Table I. Varying δ affects the activated term strongly, but has little effect on the term $bT + d$. The steep decrease in the prefactor a with δ reflects the overall decrease of the magnitude of ρ_c from A to D. However, the gap increases monotonically with δ . As discussed above, this trend is already apparent from the slope of ρ_c just above T_c . For the YBCO_{6,7} crystal, the fit gives $a = 3.93 \text{ } \Omega \text{ cm K}$ and $\Delta = 60 \text{ K}$.

Because the magnitude of ρ_c is so large, charge transport between adjacent layers is more appropriately described as tunneling between metallic planes, instead of the usual band conduction. The tunneling current has been calculated by Kumar and Jayannavar¹⁴ and by Ioffe *et al.*,¹⁵ using conventional Fermi-liquid description. However, the predicted behavior $\rho_c \sim 1/\tau$ does not seem in accord with experiment (τ is the lifetime within the plane). The tunneling amplitude was recently discussed by Clarke, Strong, and Anderson¹⁶ in a model with spin-charge separation. At present, however there appears to be little understanding of how a steeply increasing ρ_c may coexist with a linearly decreasing “metallic” ρ_{ab} in such a large class of cuprates. The MR experiments may provide further insight into this problem.

Ioffe *et al.*¹⁵ have discussed paraconductivity contributions that may lead to an increase in ρ_c above T_c . Strong fluctuations into the three-dimensional (3D) superconducting state suppress the single-particle density of states at the Fermi level and reduce the c -axis current. The effect of field on the fluctuations has been calculated.¹⁷ Recently, Nakao *et al.*¹⁸ have interpreted their negative MR experiments in

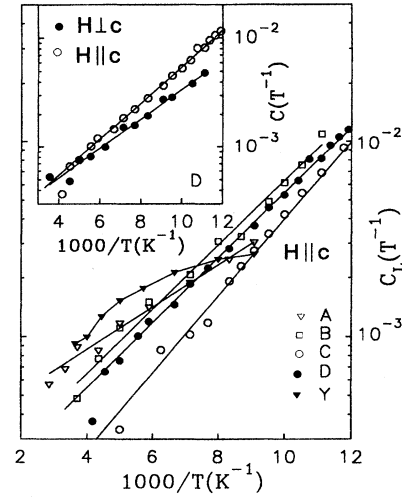


FIG. 4. (Main panel) Temperature dependence of the MR coefficient $C_L(T)$ defined by $\Delta\rho_c/\rho_c = -[C_L(T)B]^2$ (for longitudinal fields) in Bi 2212 (A, B, C, and D) and YBCO_{6,7} (sample Y). The data for Bi 2212 follows the activated form $C_L = C_{L0} \exp(U_L/T)$ (Table I). (The data for YBCO do not fit this form.) In the inset, the coefficient in longitudinal field ($\mathbf{H} \parallel c$) is compared with that in transverse field ($\mathbf{H} \perp c$). U_L and $U_T = 392$ and 313 K , respectively. \mathbf{J} is along c in both geometries.

Bi 2201 as evidence for field suppression of these fluctuations. However, this interpretation does not seem consistent with our experiment. Field suppression of 3D superconducting fluctuations should possess an anisotropy relative to field orientation that is of the order of the coherence-length anisotropy (>80 in Bi 2212), whereas we obtain an anisotropy of <2 for C_L . Further, the MR coefficient C_L continues smoothly into the mixed state, instead of diverging at T_c . Lastly, the steep increase in ρ_c with decreasing T (especially in samples A, B, and YBCO_{6,7} in Fig. 1) is part of a trend that greatly escalates as δ is further reduced. It seems implausible that paraconductivity suppression of the c -axis current becomes even more important in severely underdoped samples. Our conclusion is that the increase in ρ_c (and the MR term in C_L) are unrelated to paraconductivity effects. Close to T_c , true paraconducting terms represented by $-\gamma B \ln B$ indeed become resolvable¹³ (Fig. 3).

Our experiment suggests that the application of an intense field suppresses the formation of a correlated electronic state that precedes the appearance of 3D superconductivity. The existence of a barrier in this state leads to an activated form for ρ_c that is observable at temperatures as high as 300 K, depending on δ . An intense magnetic field weakens the correlated state and lowers the barrier, leading to the observed negative MR. The relatively weak anisotropy (<2) in the negative MR implies that the field couples to the order parameter of the correlated state by the Zeeman energy of the spin degrees with a small admixture of orbital effects. Thus, the spin degrees play a central role in establishing the correlated state and the gap Δ . An attractive scenario is that Δ originates from singlet-pair formation between electrons on opposite planes of a bilayer.^{9,19} An intense dc field destabilizes the singlet relative to the triplet. If we assume that a gap in the spin spectrum reduces the tunneling amplitude, then

the suppression of the singlet pairing by an applied field leads quite naturally to the observed negative MR. The need for simultaneous hopping of the spin and charge degrees for interlayer transport has been emphasized by Anderson.²⁰ Recently, Millis and Monien⁸ and Ubbens and Lee⁹ proposed that the interlayer exchange coupling in bilayer systems drives spin-gap formation in the bilayer cuprates. In 60-K YBCO_{6,7}, Uchida and co-workers⁴ have argued that the temperature (~ 200 K) at which a slight downturn in the in-plane resistivity ρ_{ab} occurs signals the opening of a pseudogap near 200 K. In a crystal of YBCO_{6,7} with $T_c = 63$ K, Homes *et al.*⁷ estimated from *c*-axis reflectivity an optical gap $2\Delta \sim 200$ cm⁻¹ (or $\Delta \sim 148$ K, compared with our estimate of 60 K in a crystal with a similar T_c). Both groups have suggested that the pseudogap may cause the increase in ρ_c in underdoped samples.

If we identify the gap we observe in both Bi 2212 and YBCO_{6,7} with the gap in the previous transport experiments, our MR results provide information on the origin of the gap,

especially the role of the spins. However, to arrive at a self-consistent picture, we need to understand how the oxygen content affects the parameters discussed. As we go from A to D (increasing δ), the overall magnitude of ρ_c appears to decrease. In contrast, the energy scales Δ and U_L (which represents the coupling energy to the external field) increase sharply. This trend seems to be the opposite of what is expected of the spin gap in, for example, the *tJ* model. It bears repeating that the negative MR discussed here is only weakly dependent on the field direction, especially at high temperatures. This seems to us to be very strong evidence that the spin degrees play the central role in creating the barrier to interplane charge transport in the two bilayer cuprates investigated.

We acknowledge very helpful discussions with P. W. Anderson, P. A. Lee, S. Strong, and S. Uchida. This research was supported by the National Science Foundation through the DMR-MRG program (Grant No. DMR 922 4077).

-
- ¹S. J. Hagen, T. W. Jing, Z. Z. Wang, J. Horvath, and N. P. Ong, *Phys. Rev. B* **37**, 7928 (1988).
²D. A. Brawner, Z. Z. Wang, and N. P. Ong, *Phys. Rev. B* **40**, 9329 (1989).
³T. Ito, H. Takagi, S. Ishibashi, T. Ido, and S. Uchida, *Nature (London)* **350**, 596 (1991).
⁴T. Ito, K. Takenaka, and S. Uchida, *Phys. Rev. Lett.* **70**, 3995 (1993).
⁵B. Bucher, P. Steiner, J. Karpinski, E. Kaldis, and P. Wachter, *Phys. Rev. Lett.* **70**, 2012 (1993).
⁶J. W. Loram, K. A. Mirza, J. R. Cooper, and W. Y. Liang, *Phys. Rev. Lett.* **71**, 1740 (1994).
⁷C. C. Homes, T. Timusk, R. Liang, D. A. Bonn, and W. N. Hardy, *Phys. Rev. Lett.* **71**, 1645 (1993).
⁸A. J. Millis and H. Monien, *Phys. Rev. Lett.* **70**, 2810 (1993).
⁹Menke U. Ubbens and Patrick A. Lee, *Phys. Rev. B* **50**, 438 (1994).
¹⁰C. Kendziora, L. Forro, D. Mandrus, J. Hartge, P. Stephens, L. Mihaly, R. Reeder, D. Moecher, M. Rivers, and S. Sutton, *Phys. Rev. B* **45**, 13 025 (1992).
¹¹G. Briceño, M. F. Crommie, and A. Zettl, *Phys. Rev. Lett.* **66**, 2164 (1991).
¹²J. H. Cho, M. P. Maley, S. Fleshler, A. Lacerda, and L. N. Bulaevskii, *Phys. Rev. B* **50**, 6493 (1994).
¹³Y. F. Yan, J. M. Harris, P. Matl, and N. P. Ong (unpublished).
¹⁴N. Kumar and A. M. Jayannavar, *Phys. Rev. B* **45**, 5001 (1992).
¹⁵L. B. Ioffe, A. I. Larkin, A. A. Varlamov, and L. Yu, *Phys. Rev. B* **47**, 8936 (1993).
¹⁶David G. Clarke, S. P. Strong, and P. W. Anderson, *Phys. Rev. Lett.* **72**, 3218 (1994).
¹⁷V. V. Dorin, R. A. Klemm, A. A. Varlamov, A. I. Buzdin, and D. V. Livanov, *Phys. Rev. B* **48**, 12 951 (1993).
¹⁸K. Nakao, K. Takamuku, K. Hashimoto, N. Koshizuka, and S. Tanaka, *Physica B* **201**, 262 (1994).
¹⁹B. L. Altshuler and L. B. Ioffe, *Solid State Commun.* **82**, 253 (1992).
²⁰P. W. Anderson, *Science* **256**, 673 (1992); *Phys. Rev. Lett.* **67**, 3844 (1991).